Model Predictive Control of PV Sources in a Smart DC Distribution System: Maximum Power Point Tracking and Droop Control

Mohammad B. Shadmand, *Student Member, IEEE*, Robert S. Balog, *Senior Member, IEEE*, and Haitham Abu-Rub, *Senior Member, IEEE*

***Abstract*—In a dc distribution system, where multiple power sources supply a common bus, current sharing is an important issue. When renewable energy resources are considered, such as photovoltaic (PV), dc/dc converters are needed to decouple the source voltage, which can vary due to operating conditions and maximum power point tracking (MPPT), from the dc bus voltage. Since different sources may have different power delivery capacities that may vary with time, coordination of the interface to the bus is of paramount importance to ensure reliable system operation. Further, since these sources are most likely distributed throughout the system, distributed controls are needed to ensure a robust and fault tolerant control system. This paper presents a model predictive control-based MPPT and model predictive control-based droop current regulator to interface PV in smart dc distribution systems. Back-to-back dc/dc converters control both the input current from the PV module and the droop characteristic of the output current injected into the distribution bus. The predictive controller speeds up both of the control loops, since it predicts and corrects error before the switching signal is applied to the respective converter.**

***Index Terms*—DC microgrid, droop control, maximum power point tracking (MPPT), model predictive control (MPC), photovoltaic (PV), photovoltaic systems.**

I. Introduction

REDUCTION in the cost of photovoltaic (PV) cells has increased the interest in using renewable energy sources. In the past decade, utilization of renewable energy sources has increased with 60% annual growth in the installed capacity of PV systems from 2004 to 2009, and 80% in 2011 [1]. Direct current (dc) electrical systems are also gaining popularity due in part to high efficiency, high reliability, and ease of interconnection of the renewable sources compared to alternating current (ac) systems [2], [3]. DC microgrids have been proposed to improve point-of-load energy availability and to integrate disparate renewable energy sources with energy storage [4]. Various renewable energy sources such as PV systems have natural dc couplings; therefore, it is more efficient to connect these sources directly to dc microgrid by using dc/dc converters.

A dc microgrid system with distributed PV and centralized battery storage, illustrated in Fig. 1, is an attractive technology solution for communities to "go green" while simultaneously ensures reliable electricity. The PV arrays can delivery power to the system through a dc/dc converter boosting the output voltage. A maximum power point tracking (MPPT) control technique is required for the PV system to operate at the maximum power point [5]–[7] but produces output voltage that is not constant. Thus, a second dc/dc converter is added to control the current and voltage fed into the dc bus [8]. Although power from the PV is now processed twice, dc/dc converters have very high efficiency and the back-to-back converters (see Fig. 1) would have comparable, if not better efficiency, than ac systems based on a contemporary, best-in-class inverter of comparable power rating [9]–[11].

This paper presents enhanced MPPT of PV systems by means of model predictive control (MPC) [12] techniques. One of the main contributions of this paper is enhancement of the Perturb & Observed (P&O) [5] method through a fixed step predictive control under measured fast solar radiation variation. Comparing the developed technique to the conventional P&O method shows the significant improvement in the PV system performance.

In a dc microgrid system where multiple PV source converters supply the same bus, current sharing is an important consideration [2]. Theoretically, identical supply converters will share the load current equally. However, mismatches in components and feedback networks as well as different impedances at different locations on the dc bus can cause imbalance in current sharing. If significant, this imbalance can result in overload and thermal stresses, which could jeopardize system reliability. The reliability of a single-bus dc system can be improved by using autonomous local controls rather than a central controller [13]. Droop control is one of such control technique that controls the output current from the source in response to the sensed bus voltage [14]. Since no communication is needed to coordinate controllers, the system is robust and cyber secure [15]. The second contribution of this is to develop the conventional droop control methodology by means of MPC for smart dc distribution systems. The developed droop control by MPC proposed in this paper enables a stable process control due to the nature of MPC that is predicting the error before the control signal applied to the converter.

Manuscript received March 5, 2014; revised August 2, 2014; accepted August 2, 2014. Date of publication November 5, 2014; date of current version November 20, 2014. This work was supported by the National Priorities Research Program from the Qatar National Research Fund (a Member of Qatar Foundation) under Grant 4-077-2-028. Paper no. TEC-00167-2014.R1.

M. B. Shadmand and R. S. Balog are with the Renewable Energy and Advanced Power Electronics Research Laboratory, Department of Electrical and Computer Engineering, Texas A&M University, College Station, TX 77843 USA (e-mail: mohamadshadmand@gmail.com; robert.balog@ieee.org).

H. Abu Rub is with the Department of Electrical Engineering, Texas A&M University at Qatar, Doha 23874, Qatar (e-mail: haitham.abu-rub@qatar.tamu.edu).

Color versions of one or more of the figures in this paper are available online at http://ieeexplore.ieee.org.

Digital Object Identifier 10.1109/TEC.2014.2362934

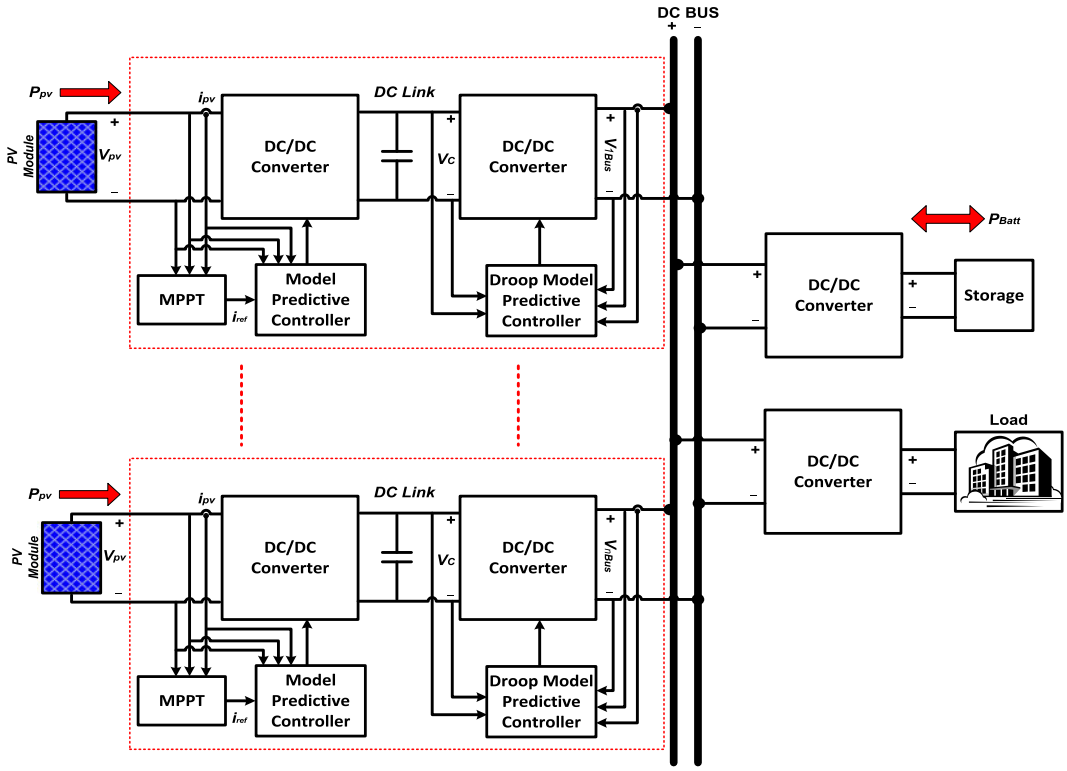

Fig. 1. Multiple-sourced dc distribution system with central storage.

Fig. 1 illustrates the general schematic of the proposed smart dc microgrid. Multiple PV arrays using model predictive control-based maximum power point tracking (MPC-MPPT) to supply power through a model predictive control-based droop (MPC-DROOP) converter into the dc distribution bus is presented. According to the availability of power from PV sources, the MPC-DROOP adjusts the droop characteristics of the dc/dc converter. In practice, the MPC-MPPT and MPC-DROOP would be integrated into a single system component, delineated by the dotted line in Fig. 1. A dc bus system with three PV sources was developed using MATLAB/Simulink and dSPACE DS1103 to verify the controls.

II. Principles of Fixed Step MPC

Application of MPC in power electronics with low switching frequency dates back to the 1980s for high-power applications [16]. Since high switching frequencies for the MPC algorithm required long calculation time, widespread adoption was not feasible at that time. In the past decade, with the improvement of high-speed microprocessors, interest in the application of MPC in power electronics with high switching frequency has increased considerably [12], [17]–[20].

The main characteristic of MPC is predicting the future behavior of the desired control variables [12] until a predefined horizon in time. The predicted variables will be used to obtain the optimal switching state by minimizing a cost function. The model used for prediction is a discrete-time model, which can be presented as a state-space model as follows [21]:

$$x(k+1) = Ax(k) + Bu(k) \quad (1)$$

$$y(k) = Cx(k) + Du(k). \quad (2)$$

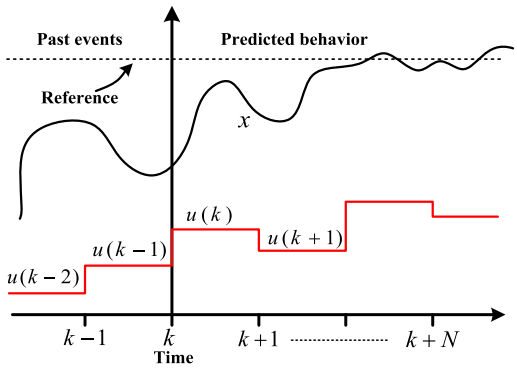

Fig. 2. MPC principle of working.

Then, a cost function that takes into consideration the future states, references and future actuations can be defined as

$$g = f(x(k), u(k), \ldots, u(k+N)). \quad (3)$$

The defined cost function g should be minimized for a predefined horizon in time N; the result is a sequence of N optimal actuations where the controller only applies the first element of sequence

$$u(k) = [1 \quad 0 \quad \cdots \quad 0] \arg\min_u g. \quad (4)$$

At each sampling time, the optimization problem is solved again by using a new set of measured data to obtain a new sequence of optimal actuation. The MPC principle of working is illustrated graphically in Fig. 2. As it is shown that by using the measured information and system model until time k, the

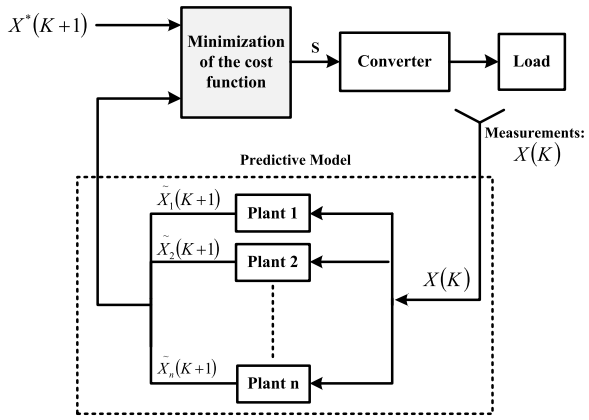

Fig. 3. MPC general schematic for power electronics converters.

future value of the system state is predicted until time $(k+N)$ in horizon. Then, the optimal actuation is calculated by optimizing the cost function (3).

The MPC for power electronics converters can be designed using the following steps [12]:

1) modeling of the power converter identifying all possible switching states and its relation to the input or output voltages or currents;
2) defining a cost function that represents the desired behavior of the system;
3) obtaining discrete-time models that allow one to predict the future behavior of the variables to be controlled.

The general scheme of MPC for power electronics converters is illustrated in Fig. 3 [12]. In this scheme, measured variables, $X(K)$, are used in the model to calculate predictions, $\tilde{X}(K+1)$, of the controlled variables for each one of the N possible actuations, that is, switching states, voltages, or currents. Then these predictions are evaluated using a cost function, which considers the reference values, $X^*(K+1)$, design constraints, and the optimal actuation, S, is selected and applied to the converter. The general form of the cost function, g, subject to minimization can be formulated as

$$\begin{aligned} g = & [\tilde{X}_1(K+1) - X_1^*(K+1)] \\ & + \lambda_1[\tilde{X}_2(K+1) - X_2^*(K+1)] \\ & + \cdots + \lambda_n[\tilde{X}_n(K+1) - X_n^*(K+1)] \end{aligned} \tag{5}$$

where λ is the weighting factor for each objective. To select the switching state, which minimizes the cost function g, all possible states are evaluated and the optimal value is stored to be applied next.

The power converter can be from any topology and number of phases, while the generic load shown in Fig. 3 can represent an electrical machine, the grid, or any other active or passive load. In this paper, the flyback power converter topology has been selected for MPPT and droop control.

III. Maximum Power Point Tracking using Model Predictive Control

The low conversion efficiency of PV cells is an obstacle to the growth of PV systems [22]. MPPT ensures that the maximum available solar energy is harnessed from the solar modules [23]–[27].

Many MPPT methods have been suggested over the past few decades; the relative merits of these various approaches are discussed in [5]. The critical operating regime is low insolation. Capturing all of the available solar power during low-insolation periods can substantially improve the system performance. An effective MPPT controller and converter can use available energy to significantly reduce the amount of installed PV.

Considering the MPPT techniques listed in [5], candidate techniques include incremental conductance [28], P&O [29], fractional open-circuit voltage [30], and best fixed voltage [31]. Each approach has certain advantages and disadvantages for the present application.

P&O is a well-known technique with relatively good performance; however, P&O method cannot always converge to the true maximum power point. Also, P&O is relatively slow, which limits its ability to track transient insolation conditions. The main contribution of this section is to improve the P&O method performance by predicting the error one step in horizon through MPC technique. The proposed method has faster response than conventional P&O under rapidly changing atmospheric conditions.

A flyback converter is chosen as a dc/dc converter. P&O determines the reference current for the MPC, which determines the next switching state. This technique predicts the error of the next sampling time and based on the optimization of the cost function g, illustrated in Fig. 6, the switching state will be determined. The inputs to the predictive controller are the PV system current and voltage, and the reference current.

By using the discrete-time set of equations, the behavior of control variable can be predicted at the next sampling time $k+1$. The proposed methodology is based on the fact that the slope of the PV array power curve is zero at the predicted MPP, positive on the left, and negative on the right of the predicted MPP. In continuous conduction mode, the discrete-time set of equations of the flyback converter shown in Fig. 4 is given by (6) and (7) when switch is "ON" and (8) and (9) when switch is "OFF" [32]

$$i_{\mathrm{PV}}(k+1) = \frac{T_S}{L_m} v_{\mathrm{PV}}(k) + i_{\mathrm{PV}}(k) \tag{6}$$

$$v_C(k+1) = \left(1 - \frac{T_S}{RC}\right) v_C(k) \tag{7}$$

$$i_{\mathrm{PV}}(k+1) = i_{\mathrm{PV}}(k) - \frac{T_S}{L_m n} v_C(k) \tag{8}$$

$$v_C(k+1) = \frac{T_S}{nC} i_{\mathrm{PV}}(k) + \left(1 - \frac{T_S}{RC}\right) v_C(k). \tag{9}$$

The PV current $i_{\mathrm{pv}}(k+1)$ is determined from (6), (8) and the reference current, i_{ref}, found using the procedure illustrated in Fig. 5. The cost function for the MPC algorithm is

$$g_{S=0,1} = \left| i_{\mathrm{PV}_{S=0,1}}(k+1) - i_{\mathrm{ref}} \right|. \tag{10}$$

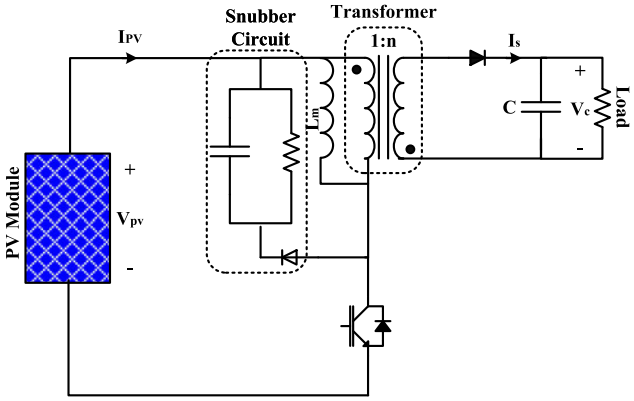

Fig. 4. Flyback converter with snubber circuit.

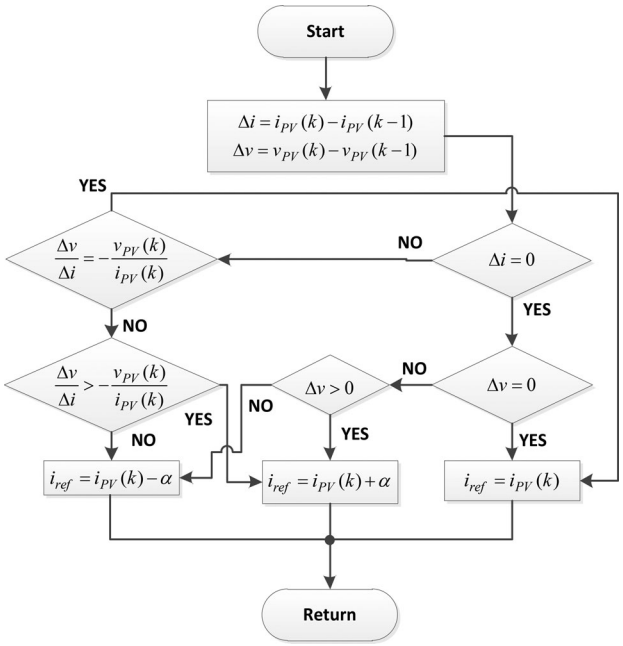

Fig. 5. MPC procedure to determine reference current using P&O.

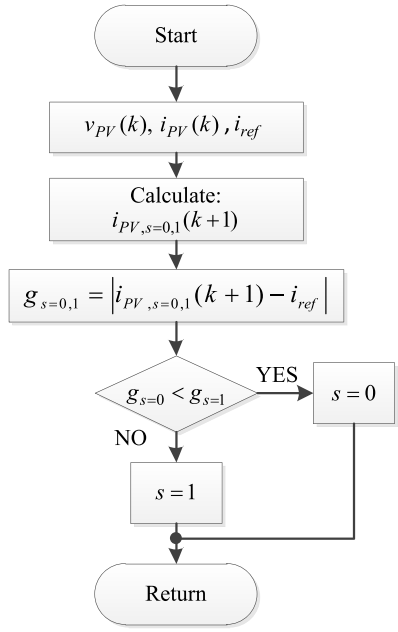

Fig. 6. MPC-MPPT procedure.

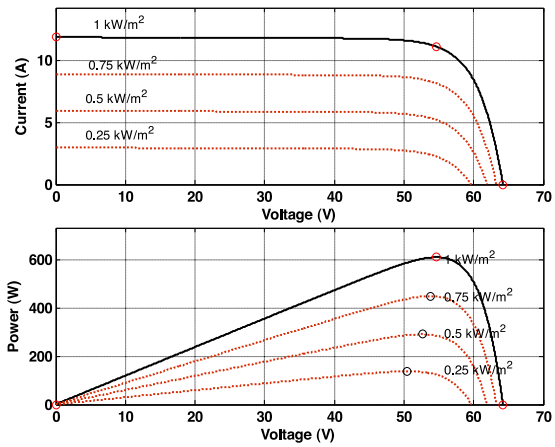

Fig. 7. *I–V* and *P–V* characteristics of the array.

The switching state for the MPPT controller is determined by minimizing the cost function g using the procedure in Fig. 6.

In this paper, we consider MPC-MPPT for one step in the horizon. Generalizing the concept, the discrete-time equation can be extended to n-step in the horizon as follows:

$$i_{\mathrm{PV}}(k+n+1) = i_{\mathrm{PV}}(k+n) - S\frac{T_S}{L}v_{\mathrm{PV}}(k) + (1-S)\frac{T_S}{Ln}v_C(k+n) \quad (11)$$

$$v_C(k+n+1) = S\left(1 - \frac{T_S}{RC}\right)v_C(k) + (1-S)\frac{T_S}{Cn}i_{\mathrm{PV}}(k+n) \quad (12)$$

where S is the switching state and T_s is the sampling time. By increasing the number of steps to two or three, the computation time will be increased but better control performance will be achieved.

The *I–V* and *P–V* characteristic of the PV systems used in this paper for different irradiance levels are illustrated in Fig. 7. In this paper, the MPC for MPPT is compared to the commonly used P&O method. The sampling time T_s is 10 μs. Fig. 8 illustrates the simulation results of the proposed MPC and conventional P&O method. The system is tested under three irradiance level changes, the irradiance level is initially at 750 W/m^2, then decreases gradually at time 0.7 s to 500 W/m^2, and finally, there is a step change in irradiance level at time 1.5 s from 500 to 750 W/m^2. As illustrated in Fig. 8, the dynamic performance of the MPC method is better than the conventional P&O method. More specifically, by applying a step change in the irradiance at time 1.5 s, when using the proposed MPC method, the MPP is

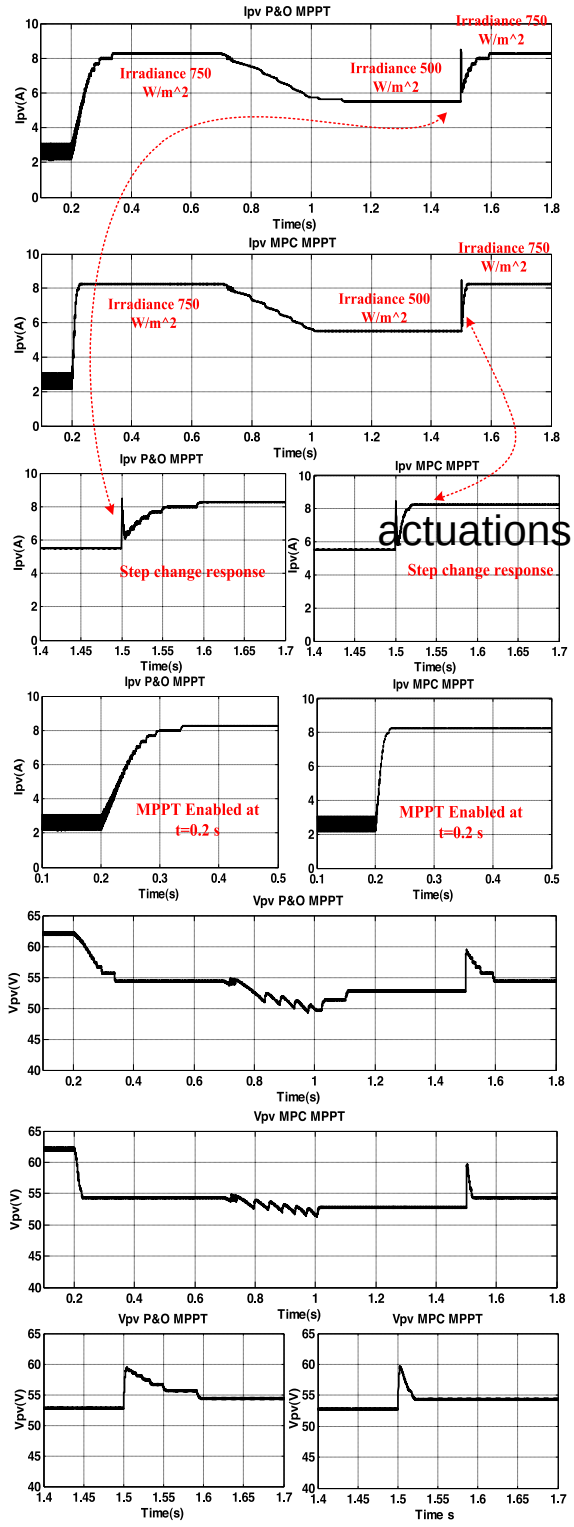

Fig. 8. Comparison of proposed MPC-MPPT to conventional P&O MPPT.

tracked at time 1.52 s; conversely when using the P&O method, the MPP is tracked at time 1.60 s. The detail descriptive plots are illustrated in Fig. 8. MATLAB/Simulink and dSPACE DS1103 is used for the experimental implementation. Figs. 9 and 10 illustrate the implementation of the MPC-MPPT, and Fig. 11 demonstrates the implementation of conventional P&O-MPPT method. As it is shown, they confirm the simulation results.

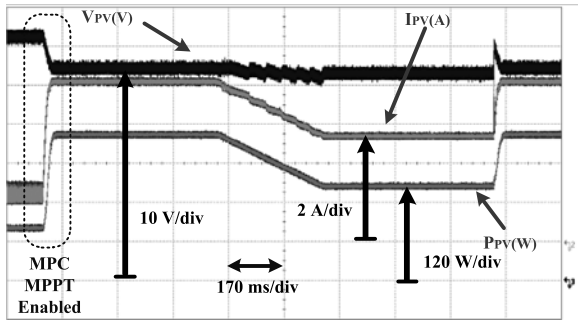

Fig. 9. PV current, voltage, and power of MPC-MPPT.

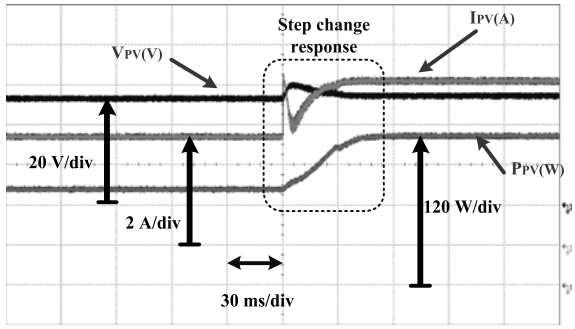

Fig. 10. PV current, voltage, and power response to step change in the irradiance from 500 to 750 W/m^2 when using MPC-MPPT method.

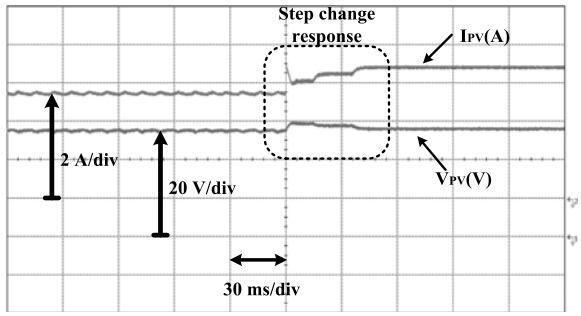

Fig. 11. PV current and voltage response to step change in the irradiance from 500 to 750 W/m^2 when using P&O-MPPT method.

IV. Droop Control Using MPC

The methods for load sharing reported in the literature fall into two groups: active sharing and droop control [33], [34].

Active current-sharing techniques involve a control structure and a method of programming individual converters with a reference current. One implementation is to use a master/slave configuration such that one dc source is designated as the *master* and is used to control the bus voltage.

The remaining dc sources, designated as *slaves*, operate as current sources. This strategy produces a stiff bus voltage and controlled load dispatch at each source. There are two main limitations of this technique: High-speed communication is required and a single point failure can disable the entire system [35]. In practice, active current-sharing techniques are best suited for physically small systems, such as paralleled voltage regulator module applications. If the topology were fixed and known *a priori*, more sophisticated controls such as interleaving can be used to reduce ripple [36].

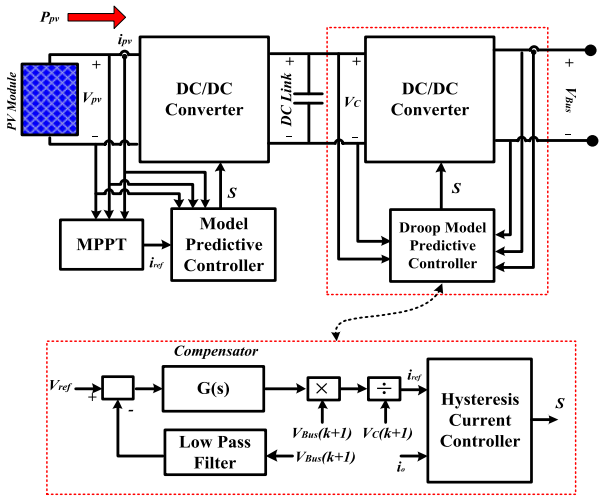

Fig. 12. Droop MPC control of the dc/dc converters.

In droop control, the output voltage of the source drops as current increases. This is a form of local control since converters autonomously share load current by sensing the local bus voltage. Droop control can be as simple as a series resistance or a more efficient closed-loop controller such as a phase-angle controller in a rectifier source converter. This scheme has been proposed for use in large-scale distributed systems [37] with dynamically changing topologies since it supports plug-and-play reconfiguration and system scaling and is robust to component failures.

In this paper, MPC is used for the droop control. MPC can forecast the error using the model of the system behavior, thus speed up stabilization process. In the proposed control scheme by using the predicted parameters and locally measured reference voltage, the reference current for each parallel converters is determined. Consequently, no communication between converters is required; as a result, the reliability of the system increases. Then, the determined reference current is used as an input to a hysteresis current controller [38] for tracking the reference current and generating the switching signal. The complete control procedure is illustrated in Fig. 12. Since the second dc/dc converter for droop control is flyback converter, the discrete-time model derived in previous section for MPPT can be used here.

The predicted variables I_o and $V_{\rm Bus}$ are the current and voltage at the output terminals of the converter at next sampling time. The voltage at the output, the bus voltage, is low-pass filtered and used to close a feedback loop. The droop gain K converts the voltage error into a current command for the source converter; it is included in the compensator block in Fig. 12. Assuming the converter current perfectly tracks the reference current, the steady-state droop relationship is

$$I_{\rm ref} = K(V_{\rm ref} - v_{\rm Bus}). \tag{13}$$

The proposed distributed system controlled by droop MPC is inherently robust because droop control automatically shares current among the available converters without the need for a central controller to redispatch the source converters. If a converter turns off or fails, the remaining converters sense a decrease in bus voltage and increase their respective output current to compensate for the lost source.

Consider a system (see Fig. 13) comprised of five PV arrays. Each PV source converter has a load-line that describes the *V–I* terminal characteristics (see Fig. 13). Assuming negligible bus impedance, the solution to the base case (where all converters are operational) results in the bus voltage $V_{\rm OP1}$ with each converter supplying $I_{\rm OP1}$ current. The analytical solution for the operating point is found by solving the load-flow equations for n source converters and m constant-power loads

$$V_{{\rm oc},n} - I_n \frac{1}{K_n} = V_{\rm bus} \forall n, \sum_n I_n = \sum_m \frac{P_m}{V_{\rm bus}}. \tag{14}$$

Contingency analysis is shown graphically in Fig. 13. As the number of source converters decreases, the bus voltage drops. Since the load is now shared by fewer sources, the current from each remaining source increases. It is observed that the droop gain is the slope of the *V–I* curve and modifies the actual source impedance. So a simple model for a source converter is

$$V_s = V_{\rm oc} - \frac{1}{K} i_s \tag{15}$$

where the droop gain K can be defined in terms of a resistance $K = 1/R_{\rm droop}$.

Although droop control can be as simple as a series resistance, a more energy efficient choice is a closed-loop controller, such as MPC used in this paper.

The bus voltage can sag for a number of reasons such as partial loss of generation, increase in load, or topological reconfiguration. The *P–V* curve is a useful tool to visualize the operation of a power system. Fig. 14 illustrates a family of the familiar *P–V* system curve. Maximum power transmission occurs at the nose where the source impedance and load impedance are equal. In a dc system, the bus voltage drops as the load increases due to voltage-divider action of the source impedance and the load impedance.

A system is initially in steady state with voltage $V(t_1)$ delivering total load power of $P(t_1)$. The system impedance suddenly increases, perhaps due to a partial loss of generation or topological reconfiguration, and the operating point moves to a new *P–V* curve at time t_2. However, the voltage $V(t_2)$ is below the undervoltage limit and load is shed, moving to a new operating point on the same *P–V* curve at t_3. The time-domain waveforms in Fig. 15 reveal that these changes in operating points do not occur instantaneously. The trajectories on the two figures, however, are idealized to improve clarity of the system response and do not include the dynamics associated with the inductance of the bus, the input filter, and the constant-power dc–dc converters.

The smart dc microgrid system illustrated in Fig. 1 is implemented in MATLAB/Simulink. The case study is done for three PV array systems. The MPPT of each array is carried out using the procedure presented in previous section. In this section, two case studies will be presented to show the effectiveness of the proposed droop MPC. The first case study evaluates the dc bus voltage response to a step change in the power drained by the load from 340 to 440 W at time 0.5 s, and then from 440 to 520 W at time 0.7 s. The reference dc bus voltage is assumed 188 V in this paper. The detailed behavior during load variation of dc microgrid bus voltage and supplied power by each converter is illustrated in Fig. 16. The input PV sources are assumed to be in balance operating point; this means the solar irradiance

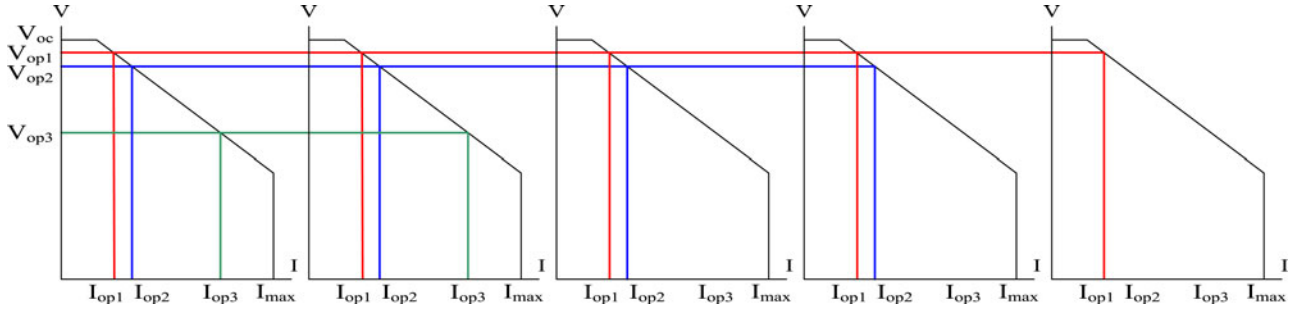

Fig. 13. Illustration of supply current sharing using droop control. The droop characteristic of the output convertor regulates the current supplied into the bus. If all supplies are identical, with the same supply capability, then current is evenly shared. Adjusting the droop characteristic can allows current to be shared automatically in arbitrary proportion, as in the case of unequal supply capabilities.

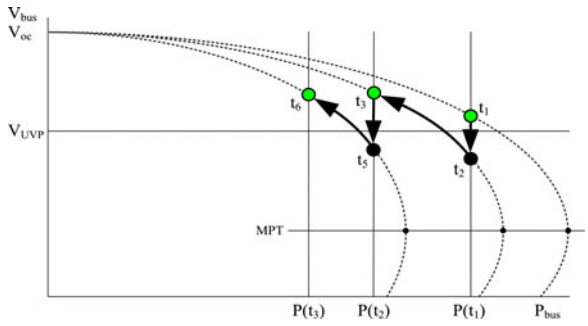

Fig. 14. *P–V* curve showing operating points as the system impedance increases and loads are interrupted.

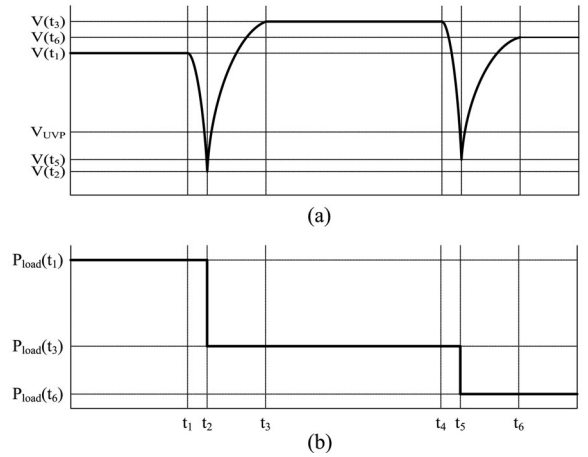

Fig. 15. Ideal bus voltage and load power as system impedance increases and loads are interrupted to prevent voltage collapse. (a) Bus voltage decreases in response to increased system impedance at t_1 to reach the operating point on the new *P–V* curve at t_2. The new bus voltage is below the UVP limit, so control action cause load to be shed, moving to a new operating point on the same *P–V* curve at t_3 with a higher bus voltage. (b) Load power in the system changes as point-of-load converters are turned OFF to reduce total system load when the bus voltage drops below the UVP.

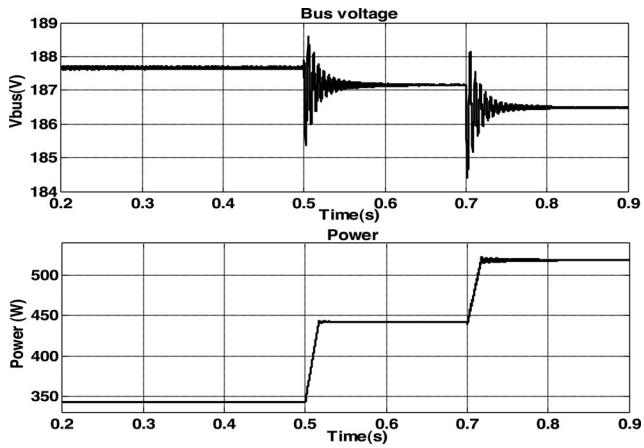

Fig. 16. Response of dc bus voltage to step changes in the power drained by load.

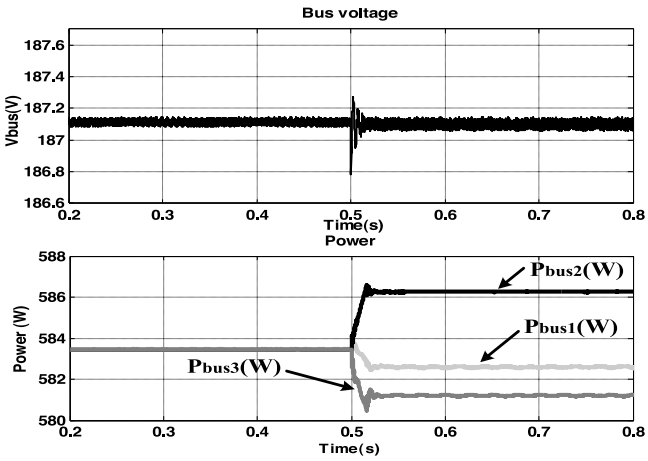

Fig. 17. Response of dc bus voltage and output power to imbalanced input PV sources.

is assumed to be constant and equal to 750 W/m^2 for all of the three first stage dc/dc converters in this case study. The bus voltage regulation has fast dynamic response to the step change in power drained by load, though the bus voltage dropped to 187.1 V at time 0.55 s and 186.5 V at time 0.75 s. Thus, as shown, the bus voltage regulation is perfectly done with 0.80% error.

The simulation results of this case study are implemented using dSPACE DS1103 and verified as shown in Fig. 18. These results demonstrate that the proposed approach is valid for a step change in the power drained by load. The second case study

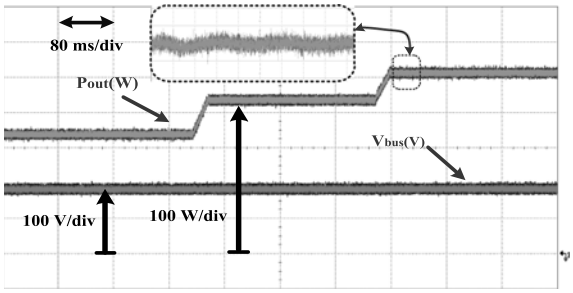

Fig. 18. Response validation of dc bus voltage to step changes in the power drained by load.

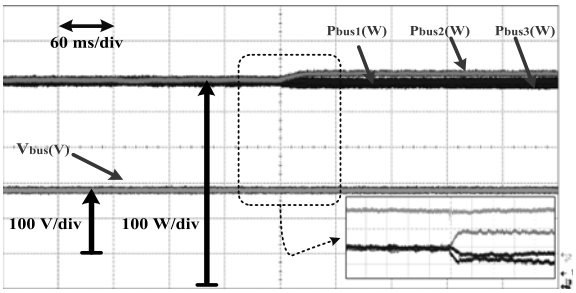

Fig. 19. Response validation of dc bus voltage and output power to imbalanced input PV sources.

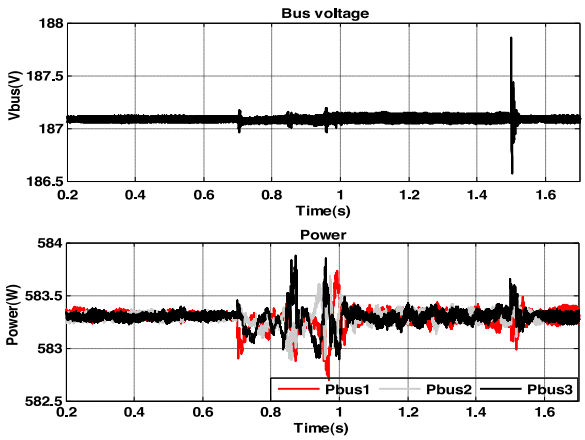

Fig. 20. Response of dc bus voltage and output power to the input PV sources of Fig. 7.

evaluates the droop MPC under imbalanced input PV sources. The solar irradiance level for all three input PV sources are 750 W/m^2 before time 0.5 s; at this time, the irradiance level of PV sources 1 and 3 dropped to 400 and 300 W/m^2, respectively, and the irradiance level of PV source 2 increased to 850 W/m^2. Fig. 17 illustrates the bus voltage and the power supplied to the bus for this case study. The implementation of the droop control is done for this case, as illustrated in Fig. 19. Fig. 20 illustrates the response of dc bus voltage and output power to the input PV sources of Fig. 8. The variation of the power supplied to the bus during the time interval 0.7 to 1.0 s is due to the gradual reduction of solar irradiance level from 750 to 500 W/m^2. Also, as illustrated earlier in Fig. 8, a step change in solar irradiance from 500 to 750 W/m^2 occurred at time 1.5 s, which is also appeared in Fig. 20.

V. Conclusion

High efficiency and easy interconnection of renewable energy sources increase interests in dc distribution systems. This paper examined autonomous local controllers in a single-bus dc microgrid system for MPP tracked PV sources. An improved MPPT technique for dc distribution system is introduced by predicting the error at next sampling time using MPC. The proposed predictive MPPT technique is compared to commonly used P&O method to show the benefits and improvements in the speed and efficiency of the MPPT. The results show that the MPP is tracked much faster by using the MPC technique than P&O method.

In a smart dc distribution system for microgrid community, parallel dc/dc converters are used to interconnect the sources, load, and storage systems. Equal current sharing between the parallel dc/dc converters and low voltage regulation is required. The proposed droop MPC can achieve these two objectives. The proposed droop control improved the efficiency of the dc distribution system because of the nature of MPC, which predicts the error one step in horizon before applying the switching signal. The effectiveness of the proposed MPPT-MPC and droop MPC is verified through detailed simulation of case studies. Implementation of the MPPT-MPC and droop MPC using dSPACE DS1103 validates the simulation results.

References

[1] Z. Peng, W. Yang, X. Weidong, and L. Wenyuan, "Reliability evaluation of grid-connected photovoltaic power systems," *IEEE Trans. Sustain. Energy*, vol. 3, no. 3, pp. 379–389, Jun. 2012.
[2] W. Baochao, M. Sechilariu, and F. Locment, "Intelligent DC microgrid with smart grid communications: Control strategy consideration and design," *IEEE Trans. Smart Grid*, vol. 3, no. 4, pp. 2148–2156, Dec. 2012.
[3] R. Majumder, "A hybrid microgrid with DC connection at back to back converters," *IEEE Trans. Smart Grid*, vol. 5, no. 1, pp. 251–259, Jun. 2013.
[4] R. Lasseter, A. Akhil, C. Marnay, J. Stephens, J. Dagle, R. Guttromson, A. S. Meliopoulous , R. Yinger, and J. Eto, "Integration of distributed energy resources. The CERTS microgrid concept," U.S. Dept. Energy, Tech. Rep. LBNL-50829, 2002.
[5] T. Esram and P. L. Chapman, "Comparison of photovoltaic array maximum power point tracking techniques," *IEEE Trans. Energy Convers.*, vol. 22, no. 2, pp. 439–449, Jun. 2007.
[6] C. Chian-Song, "T-S fuzzy maximum power point tracking control of solar power generation systems," *IEEE Trans. Energy Convers.*, vol. 25, no. 4, pp. 1123–1132, Nov. 2010.
[7] Z. Fan, K. Thanapalan, A. Procter, S. Carr, and J. Maddy, "Adaptive hybrid maximum power point tracking method for a photovoltaic system," *IEEE Trans. Energy Convers.*, vol. 28, no. 2, pp. 353–360, Apr. 2013.
[8] Y. C. Chang, C. L. Kuo, K. H. Sun, and T. C. Li, "Development and operational control of two-string maximum power point trackers in DC distribution systems," *IEEE Trans. Power Electron.*, vol. 28, no. 4, pp. 1852–1861, Apr. 2013.
[9] S. Xu, A. Q. Huang, S. Lukic, and M. E. Baran, "On integration of solid-state transformer with zonal DC microgrid," *IEEE Trans. Smart Grid*, vol. 3, no. 2, pp. 975–985, May 2012.
[10] L. Ching-Ming, P. Ching-Tsai, and C. Ming-Chieh, "High-efficiency modular high step-up interleaved boost converter for DC-microgrid applications," *IEEE Trans. Ind. Appl.*, vol. 48, no. 1, pp. 161–171, Jan. 2012.
[11] J. B. Wang, "Parallel DC/DC converters system with a novel primary droop current sharing control," *IET Power Electron.*, vol. 5, pp. 1569–1580, 2012.
[12] J. Rodriguez, M. P. Kazmierkowski, J. R. Espinoza, P. Zanchetta, H. Abu-Rub, H. A. Young, C. A. Rojas, "State of the art of finite control set model predictive control in power electronics," *IEEE Trans. Ind. Informat.*, vol. 9, no. 2, pp. 1003–1016, Jan. 2013.
[13] R. S. Balog, W. W. Weaver, and P. T. Krein, "The load as an energy asset in a distributed DC smartgrid architecture," *IEEE Trans. Smart Grid*, vol. 3, no. 1, pp. 253–260, Feb. 2012.

[14] A. Ghazanfari, M. Hamzeh, H. Mokhtari, and H. Karimi, "Active power management of multihybrid fuel cell/supercapacitor power conversion system in a medium voltage microgrid," *IEEE Trans. Smart Grid*, vol. 3, no. 4, pp. 1903–1910, Dec. 2012.
[15] F. Katiraei, R. Iravani, N. Hatziargyriou, and A. Dimeas, "Microgrids management," *IEEE Power Energy Mag.*, vol. 6, no. 3, pp. 54–65, May 2008.
[16] J. Holtz and S. Stadtfeld, "A predictive controller for the stator current vector of AC machines fed from a switched voltage source," in *Proc. Int. Power Electron. Conf.*, 1983, pp. 1665–1675.
[17] H. Abu-Rub, J. Guzinski, Z. Krzeminski, and H. A. Toliyat, "Predictive current control of voltage-source inverters," *IEEE Trans. Ind. Electron.*, vol. 51, no. 4, pp. 585–593, Jun. 2004.
[18] P. Cortes, A. Wilson, S. Kouro, J. Rodriguez, and H. Abu-Rub, "Model predictive control of multilevel cascaded h-bridge inverters," *IEEE Trans. Ind. Electron.*, vol. 57, no. 8, pp. 2691–2699, Jul. 2010.
[19] J. D. Barros, J. F. A. Silva, and E. G. A. Jesus, "Fast-predictive optimal control of NPC multilevel converters," *IEEE Trans. Ind. Electron.*, vol. 60, no. 2, pp. 619–627, Feb. 2013.
[20] H. Jiefeng, Z. Jianguo, L. Gang, G. Platt, and D. G. Dorrell, "Multi-objective model-predictive control for high-power converters," *IEEE Trans. Energy Convers.*, vol. 28, no. 3, pp. 652–663, Sep. 2013.
[21] J. Rodriguez and P. Cortes, *Predictive Control of Power Converters and Electrical Drives*. Hoboken, NJ, USA: Wiley, 2012, vol. 37.
[22] M. Kasper, D. Bortis, T. Friedli, and J. W. Kolar, "Classification and comparative evaluation of PV panel integrated DC-DC converter concepts," in *Proc. IEEE Power Electron. Motion Control Conf.*, 2012, pp. LS1e.4-1–LS1e.4-8.
[23] L. Zhigang, A. Q. Huang, and G. Rong, "High efficiency switched capacitor buck-boost converter for PV application," in *Proc. IEEE Appl. Power Electron. Conf. Expo.*, 2012, pp. 1951–1958.
[24] P. S. Shenoy, K. A. Kim, B. B. Johnson, and P. T. Krein, "Differential power processing for increased energy production and reliability of photovoltaic systems," *IEEE Trans. Power Electron.*, vol. 28, no. 6, pp. 2968–2979, Jun. 2013.
[25] J. Wei and B. Fahimi, "Maximum solar power transfer in multi-port power electronic interface," in *Proc. IEEE Appl. Power Electron. Conf. Expo.*, 2010, pp. 68–73.
[26] M. Shadmand, R. S. Balog, and H. Abu Rub, "Maximum power point tracking using model predictive control of a flyback converter for photovoltaic applications," in *Proc. IEEE Power Energy Conf. Illinois*, 2014, pp. 1–5.
[27] M. B. Shadmand, M. Mosa, R. S. Balog, and H. A. Rub, "An improved MPPT technique of high gain DC-DC converter by model predictive control for photovoltaic applications," in *Proc. IEEE Appl. Power Electron. Conf. Expo.*, 2014, pp. 2993–2999.
[28] A. Bidram, A. Davoudi, and R. S. Balog, "Control and circuit techniques to mitigate partial shading effects in photovolt. arrays," *IEEE J. Photovolt.*, vol. 2, no. 4, pp. 532–546, Oct. 2012.
[29] N. Femia, G. Petrone, G. Spagnuolo, and M. Vitelli, "Optimization of perturb and observe maximum power point tracking method," *IEEE Trans. Power Electron.*, vol. 20, no. 4, pp. 963–973, Jul. 2005.
[30] K. A. Kim, R. M. Li, and P. T. Krein, "Voltage-offset resistive control for DC-DC converters in photovoltaic applications," in *Proc. IEEE Appl. Power Electron. Conf. Expo.*, 2012, pp. 2045–2052.
[31] D. Sera, T. Kerekes, R. Teodorescu, and F. Blaabjerg, "Improved MPPT algorithms for rapidly changing environmental conditions," in *Proc. IEEE Power Electron. Motion Control Conf.*, 2006, pp. 1614–1619.
[32] R. W. Erickson and D. Maksimovic, *Fundamentals of Power Electronics*. Norwell, MA, USA: Kluwer, 2001.
[33] S. Luo, Z. Ye, R.-L. Lin, and F. C. Lee, "A classification and evaluation of paralleling methods for power supply modules," in *Proc. Power Electron. Spec. Conf.*, 1999, pp. 901–908.
[34] Z. Moussaoui, I. Batarseh, H. Lee, and C. Kennedy, "An overview of the control scheme for distributed power systems," in *Southcon Conf. Rec.*, Orlando, FL, USA, 1996, pp. 584–591.
[35] Z. Ye, D. Boroyevich, K. Xing, and F. C. Lee, "Design of parallel sources in DC distributed power systems by using gain-scheduling technique," in *Proc. Power Electron. Spec. Conf.*, 1999, pp. 161–165.
[36] X. Zhou, P.-L. Wong, P. Xu, F. C. Lee, and A. Q. Huang, "Investigation of candidate VRM topologies for future microprocessors," *IEEE Trans. Power Electron.*, vol. 15, no. 6, pp. 1172–1182, Nov. 2000.
[37] B. K. Johnson, R. H. Lasseter, F. L. Alvarado, and R. Adapa, "Expandable multiterminal DC systems based on voltage droop," *IEEE Trans. Power Del.*, vol. 8, no. 4, pp. 1926–1932, Oct. 1993.
[38] B. K. Bose, "An adaptive hysteresis-band current control technique of a voltage-fed PWM inverter for machine drive system," *IEEE Trans. Ind. Electron.*, vol. 37, no. 5, pp. 402–408, Oct. 1990.

Mohammad B. Shadmand (S'09) received the B.S. degree in electrical engineering from Qatar University, Doha, Qatar, in 2010, and the M.S. degree in electrical engineering from Texas A&M University, College Station, TX, USA, in 2012, where he is currently working toward the Ph.D. degree in electrical engineering.

He is a Researcher with the Renewable Energy and Advanced Power Electronics Research Laboratory, Texas A&M University, since 2010. His research interests include finite element analysis of high-frequency magnetic components, model predictive control, matrix converter, performance analysis of photovoltaic systems, and switching power supplies.

Mr. Shadmand was awarded second place in the IEEE Industrial Application Society Graduate Thesis Contest for his M.S. thesis in 2013.

Robert S. Balog (S'92–M'96–SM'07) received the B.S. degree in electrical engineering from Rutgers—State University of New Jersey, New Brunswick, NJ, USA, and the M.S. and Ph.D. degrees in electrical engineering from the University of Illinois at Urbana–Champaign, Urbana, IL, USA.

He was an Engineer with Lutron Electronics, Coopersburg, PA, USA, from 1996 to 1999; a Researcher with the U.S. Army Corp of Engineers, Engineering Research and Development Center, Construction Engineering Research Lab, Champaign, IL, from 2005 to 2006; a Senior Engineer at SolarBridge Technologies, Champaign, from 2006 to 2009; and then joined Texas A&M University, College Station, TX, USA, where he is currently an Assistant Professor in the Department of Electrical and Computer Engineering and Director of the Renewable Energy and Advanced Power Electronics Research Laboratory. He holds 14 issued and pending U.S. patents. His current research interests include power converters for solar energy, particularly microinverters for ac photovoltaic modules and highly reliable electrical power and energy systems, including dc microgrids.

Dr. Balog received the IEEE Joseph J. Suozzi INTELEC Fellowship in Power Electronics in 2001, and also the Rutgers School of Engineering Distinguished Engineer Award in 2011. He is a Registered Professional Engineer in Illinois. He is a Member of Eta Kappa Nu, Sigma Xi, the National Society of Professional Engineers, the American Solar Energy Society, and the Solar Electric Power Association.

Haitham Abu-Rub (M'99–SM'07) received the M.Sc. degree in electrical engineering from Gdynia Marine Academy, Gdynia, Poland, in 1990, and the Ph.D. degree in electrical engineering from the Gdansk University of Technology, Gdansk, Poland, in 1995.

For eight years, he was with Birzeit University, Birzeit, Palestine, where he was first an Assistant Professor and then an Associate Professor, and was the Chairman of the Electrical Engineering Department for four years. He is currently a Full Professor with the Department of Electrical and Computer Engineering, Texas A&M University at Qatar, Doha, Qatar. His main research interests include the electrical machine drives and power electronics.

Dr. Abu-Rub received many international prestigious awards, such as the American Fulbright Scholarship (Texas A&M University, College Station, TX, USA), the German Alexander von Humboldt Fellowship (Wuppertal University, Wuppertal, Germany), the German Deutscher Akademischer Austausch Dienst (DAAD) Scholarship (Ruhr University Bochum, Germany), and the British Royal Society Scholarship (University of Southampton, Southampton, U.K.)